Spring 3-28-2012

Blood Flow Through the Aorta in a Mouse Model of Atherosclerosis

J. Hough
Monash University

P. Assemat
Monash University

K.K.W. Siu
Monash University

J.A. Armitage
Monash University

K. Contreras
Monash University

See next page for additional authors

Blood Flow Through the Aorta in a Mouse Model of Atherosclerosis

J. Hough[1], P. Assemat[1], K. K. W. Siu[2,3], J. A. Armitage[4] , K. Contreras[1], A. Aprico[5], A. Dart[5], J. Chin-Dusting[5], K. Hourigan[1]

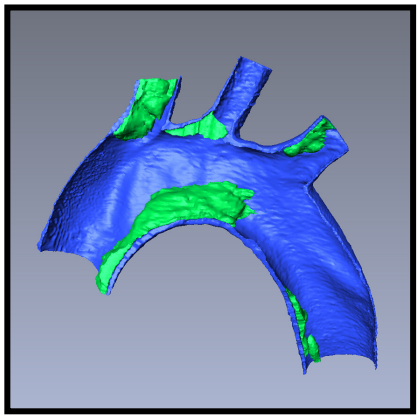

[1]Department of Mechanical and Aerospace engineering &
Division of Biological Engineering, Monash University, Melbourne, Australia
[2]Monash Biomedical Imaging, Monash University, Clayton, Australia
[3]Australian Synchrotron, Clayton Australia
[4]Department of Anatomy and Developmental Biology, Monash University, Melbourne, Australia
[5]Baker IDI Heart and Diabetes Institute, Melbourne, Australia

ECI Conference on Computational Fluid Dynamics (CFD) in Medicine and Biology / Seventh International Biofluid Mechanics Symposium

March 25-30, 2012, Crowne Plaza Dead Sea, Ein Bokek, Dead Sea, Israel

Outline of the Presentation

- Context of current research
- Atherosclerosis overview
- Computed Tomographic X-ray Velocimetry
  - Synthetic: Stenosis
  - In vitro: Thrombi
  - In vivo: Heart
- CFD
  - Idealised stenoses
  - Mouse aorta
- Conclusions

Organigram

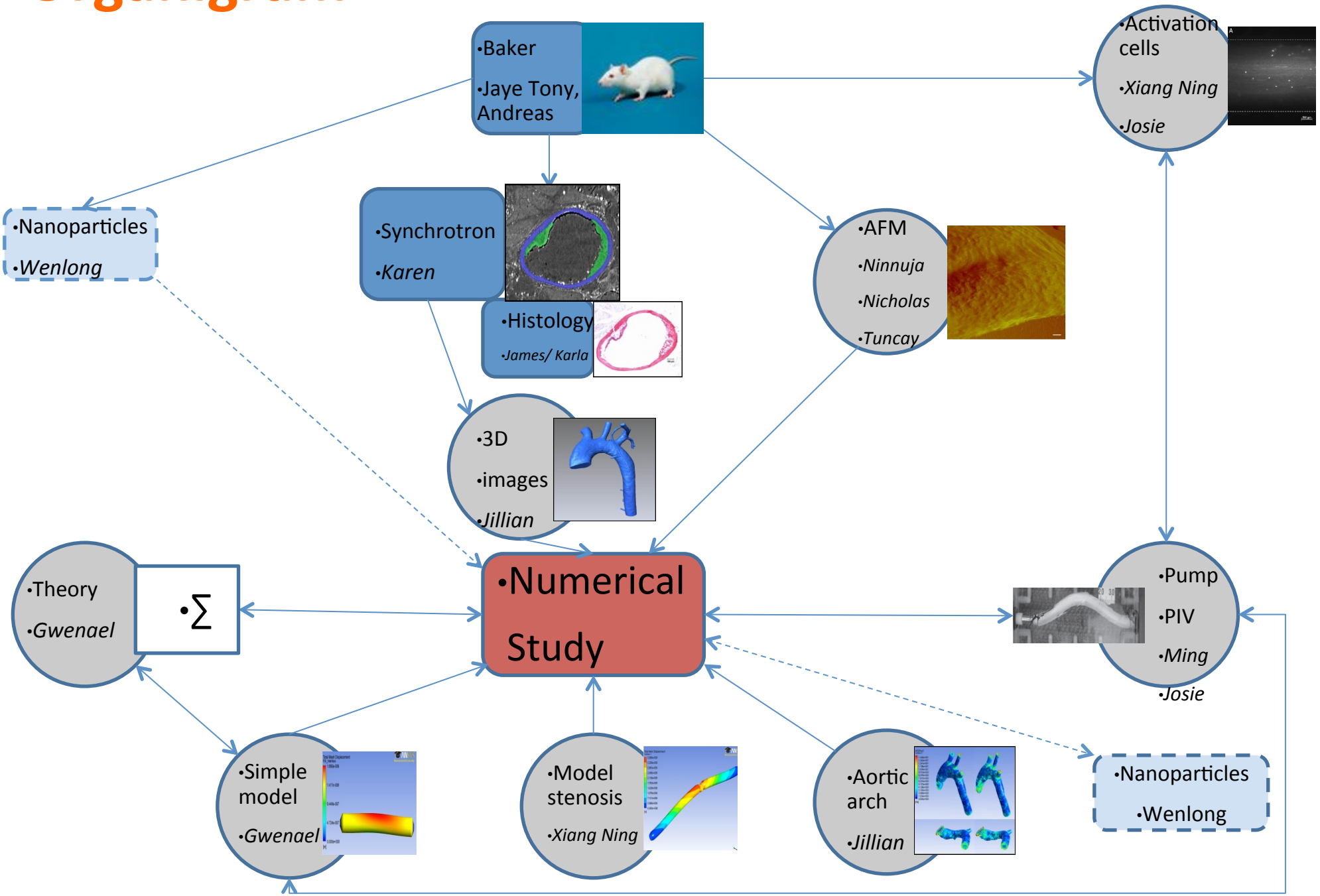
•Baker
•Jaye Tony, Andreas
•Activation cells
•Xiang Ning
•Josie
•Nanoparticles
•Wenlong
•Synchrotron
•Karen
•Histology
•James/ Karla
•AFM
•Ninnuja
•Nicholas
•Tuncay
•3D
•images
•Jillian
•Theory
•Gwenael
•∑
•Numerical Study
•Pump
•PIV
•Ming
•Josie
•Simple model
•Gwenael
•Model stenosis
•Xiang Ning
•Aortic arch
•Jillian
•Nanoparticles
•Wenlong

Outline of the Presentation

- Context of current research
- Atherosclerosis overview
- Computed Tomographic X-ray Velocimetry
    - Synthetic: Stenosis
    - In vitro: Thrombi
    - In vivo: Heart
- CFD
    - Idealised stenoses
    - Mouse aorta
- Conclusions

Sequence of progression of atherosclerosis

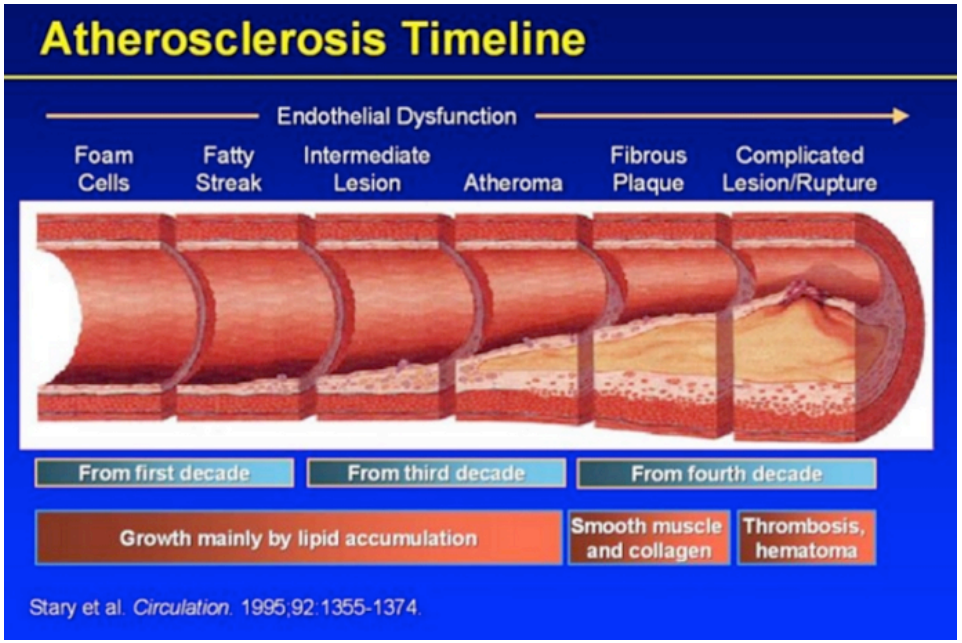

www.coastalcimt.com

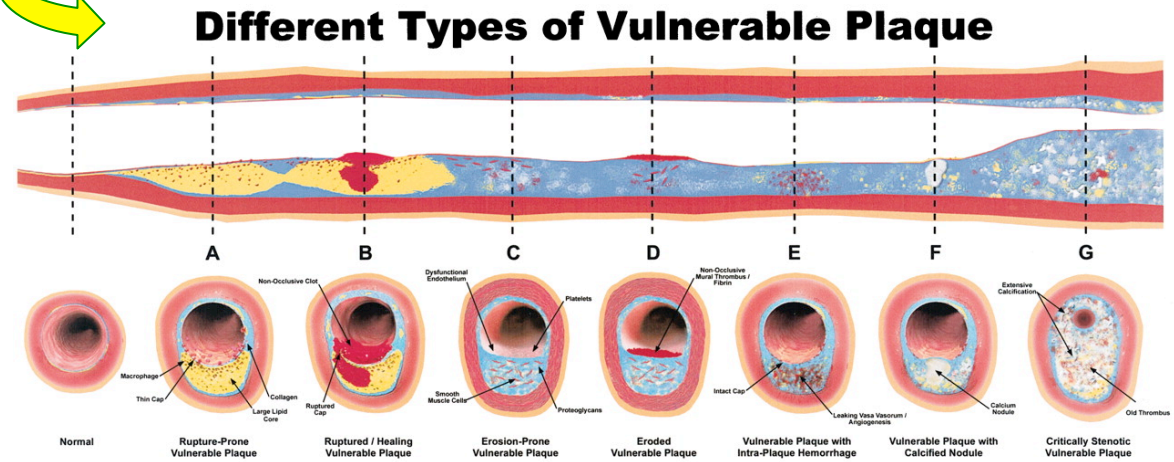

www.vp.org

Biomolecular activity in atherosclerosis

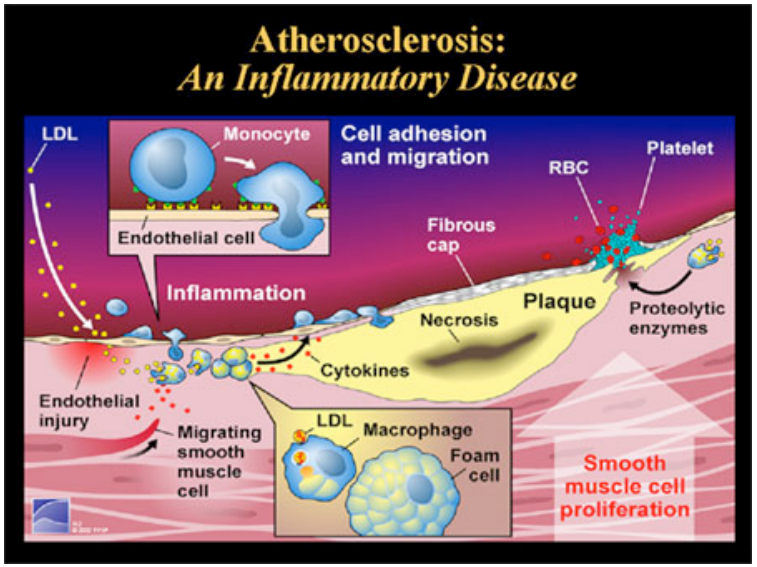

www.lancastria.net

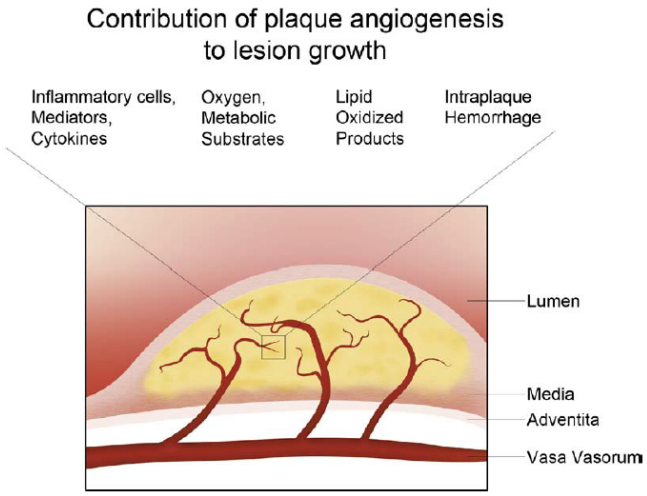

Caplice, N. & Martin, K., , J. Am. Coll. Cardiol., 3 (1 2) , 2010

Refer to review paper:

Stabilisation of atherosclerotic plaques

Position Paper of the European Society of Cardiology (ESC) Working Group on Atherosclerosis and Vascular Biology

Thrombosis and Haemostasis 2011; 106: 1–19

Seppo Ylä-Herttuala; Jacob Fog Bentzon; Mat Daeme; Erling Falk; Hector M. Garcia-Garcia; Joerg Herrmann; Imo Hoefer; J. Wouter Jukema; Rob Krams; Brenda R. Kwak; Nikolaus Marx; Marek Naruszewicz; Andrew Newby; Gerard Pasterkamp; Patrick W. J. C. Serruys; Johannes Waltenberger; Christian Weber; Lale Tokgözoglu

Outline of the Presentation

- Context of current research
- Atherosclerosis overview
- Computed Tomographic X-ray Velocimetry
    - Synthetic: Stenosis
    - In vitro: Thrombi
    - In vivo: Heart
- CFD
    - Idealised stenoses
    - Mouse aorta
- Conclusions

From PIV to Computed Tomographic X-ray Velocimetry

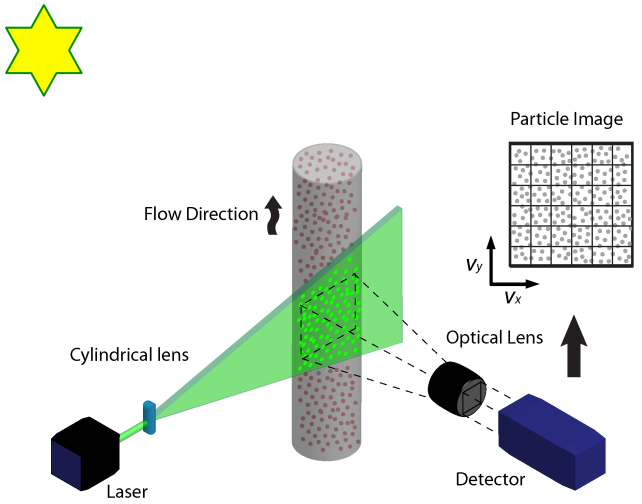

PIV with laser light

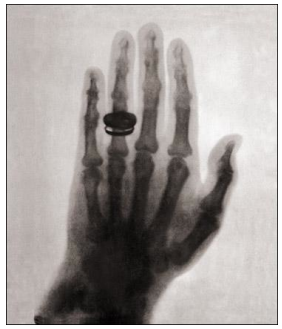

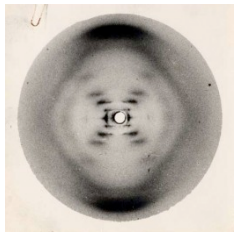

X-rays: opaque and small objects

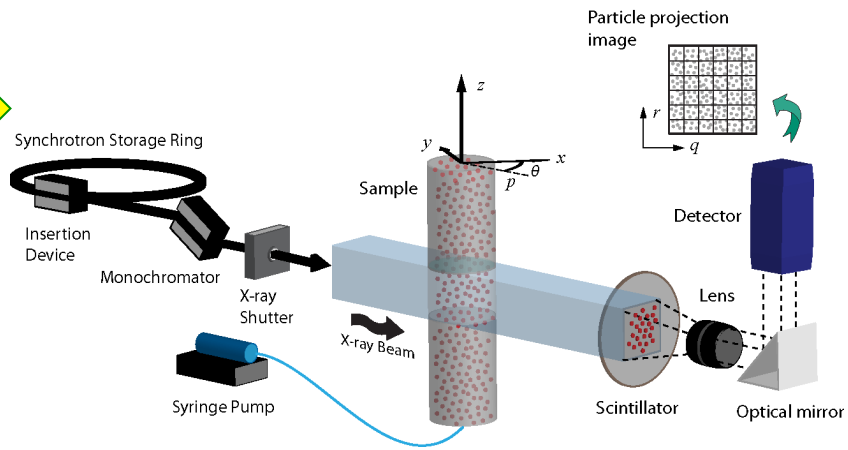

Experimental setup for CTXV

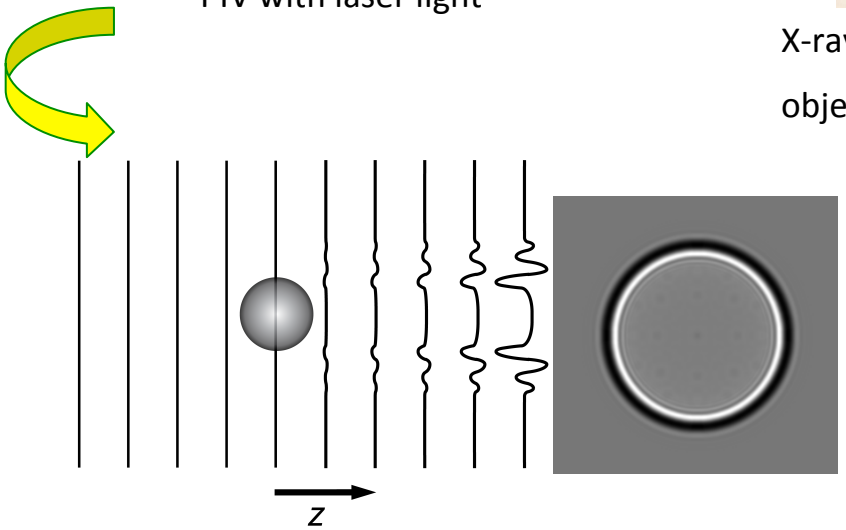

Phase contrast imaging increases signal from weakly absorbing objects

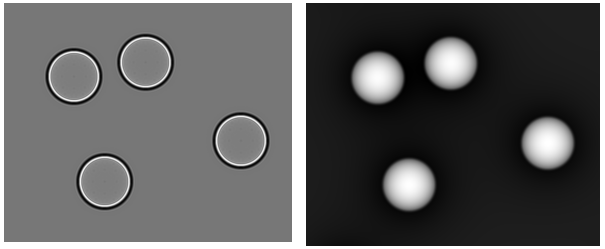

Phase retrieval algorithm allows for recovery of projected thickness

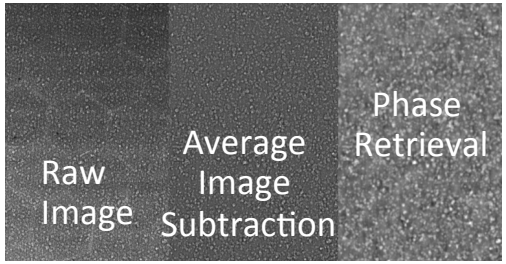

Pre-processing improves images for analysis

From PIV to Computed Tomographic X-ray Velocimetry (ctd)

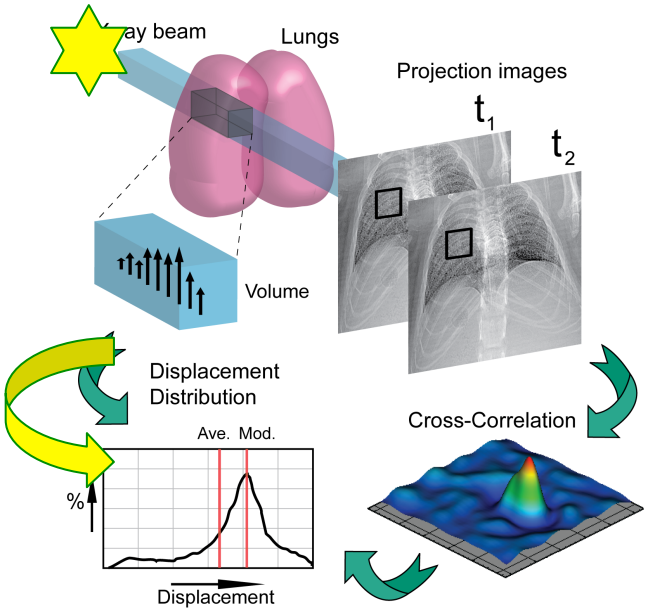

The cross-correlation contains VOLUMETRIC motion information

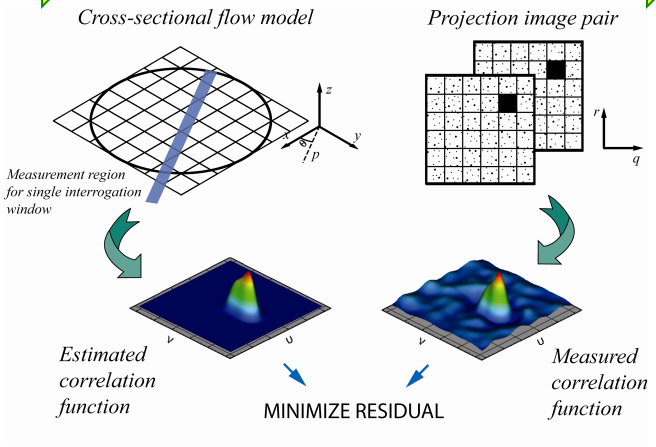

Non-linear iterative algorithm is to reconstruct the 3D velocity profile from the 2D cross-correlations

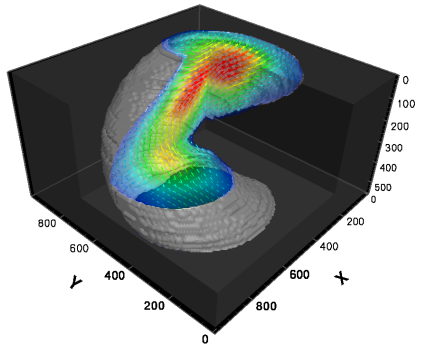

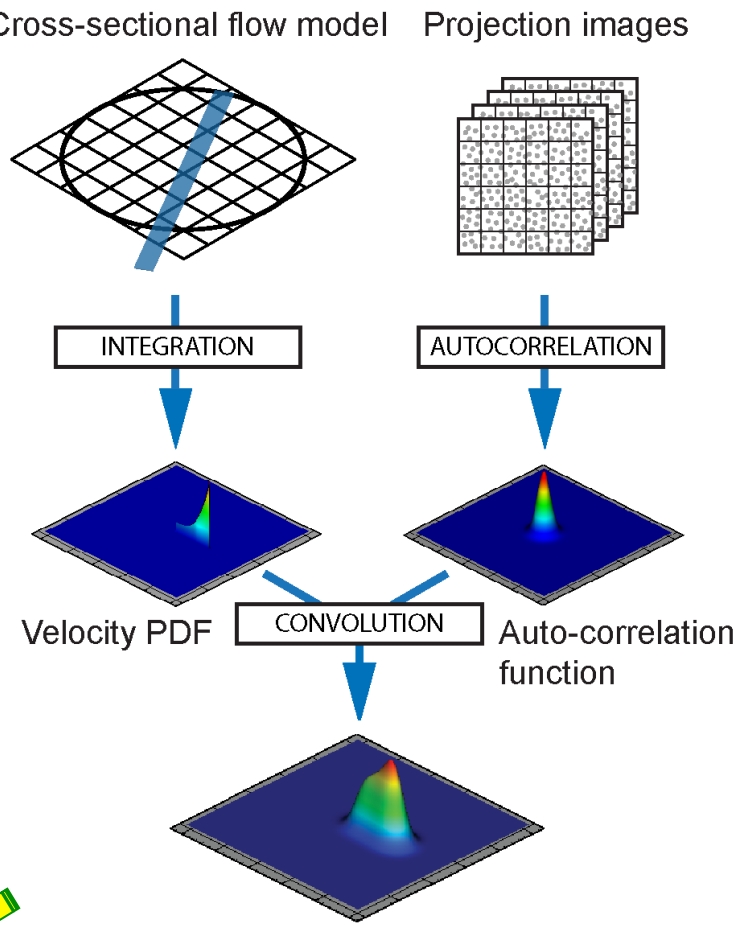

Estimated cross correlation function

Forward projection estimates cross-correlation function

Dubsky, S., Jamison, R., Higgins, S., Siu, K., Hourigan, K. & Fouras, A., *Computed Tomographic X-ray Velocimetry for simultaneous 3D measurement of velocity and geometry in opaque vessels*, Experiments in Fluids, 2012, 52:543–554.

Outline of the Presentation

- Context of current research
- Atherosclerosis overview
- Computed Tomographic X-ray Velocimetry
  - Synthetic: Stenosis
  - In vitro: Thrombi
  - In vivo: Heart
- CFD
  - Idealised stenoses
  - Mouse aorta
- Conclusions

X-ray PIV (2D) measurement of flow in a synthetic stenosed vessel

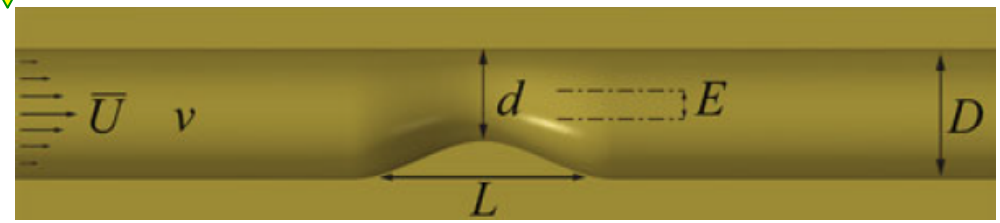

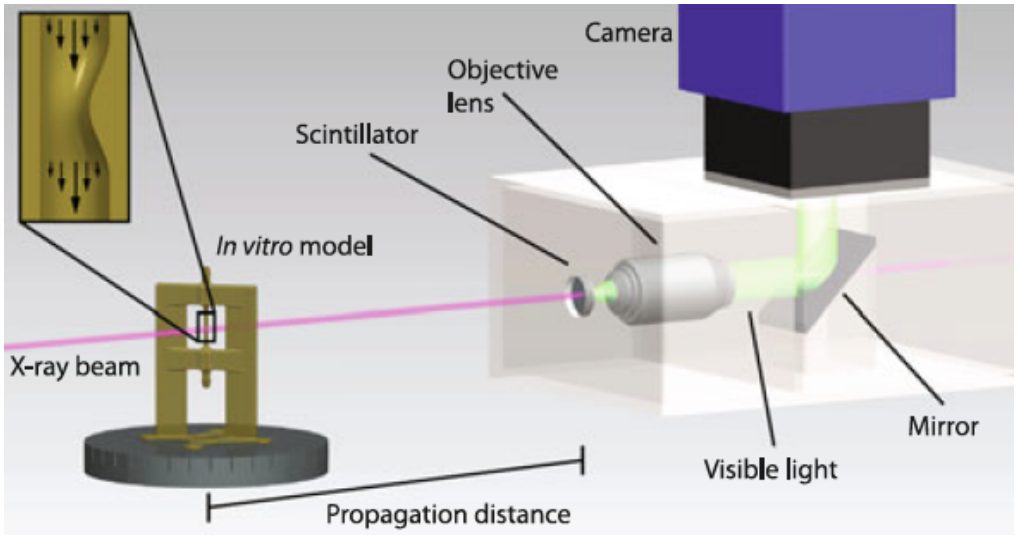

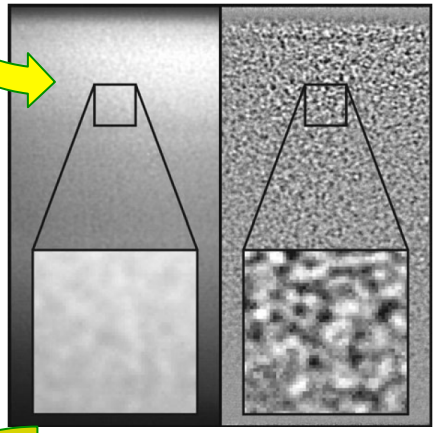

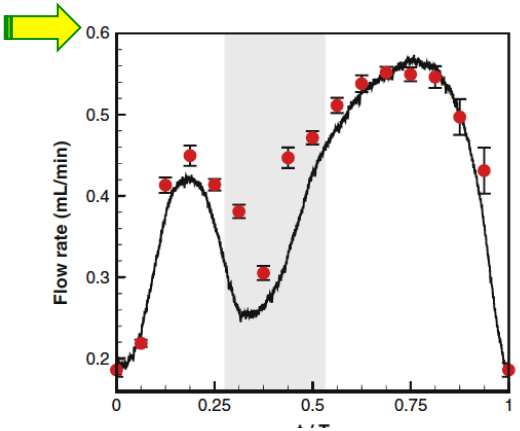

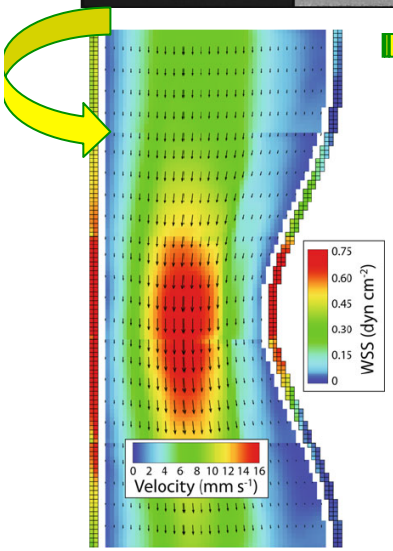

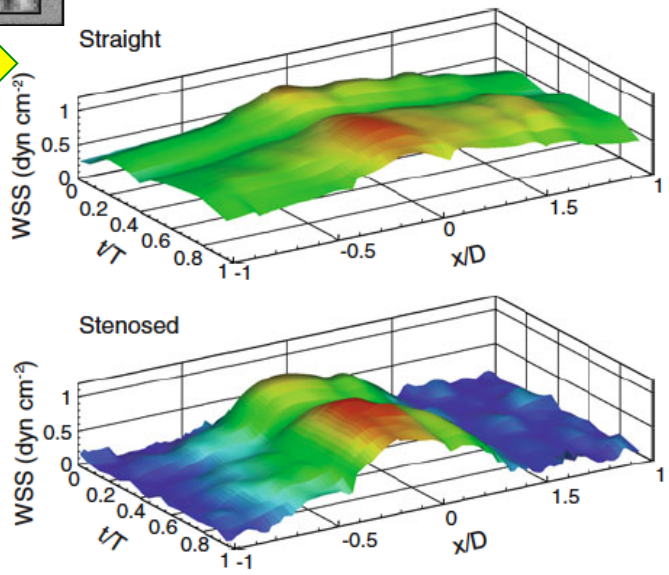

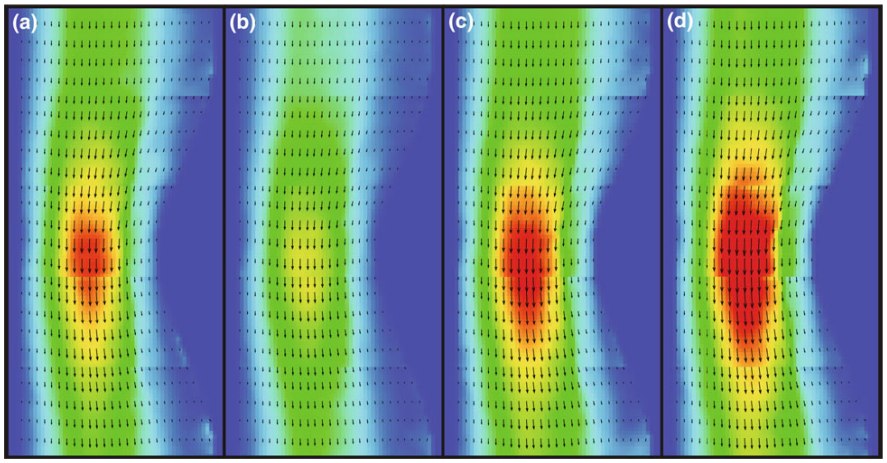

Jamison, R.A., Dubsky, S., Siu, K.W., Hourigan, K., Fouras, A., *X-ray velocimetry and haemodynamic forces within a stenosed femoral model at physiological flow rates*, Annals of Biomedical Engineering, 39 (6), 1643-1653, 2011.

Outline of the Presentation

- Context of current research
- Atherosclerosis overview
- Computed Tomographic X-ray Velocimetry
    - Synthetic: Stenosis
    - In vitro: Thrombi
    - In vivo: Heart
- CFD
    - Idealised stenoses
    - Mouse aorta
- Conclusions

The evolution of thrombi geometry

Platelets Can Promote Inflammation & Plaque Instability

Activated Platelets

Inflammatory Mediators

- CD40L
- Platelet-derived growth factor
- Platelet factor 4
- RANTES
- Thrombospondin
- Transforming growth factor-β
- Nitric Oxide

Plaque Rupture & Thrombosis

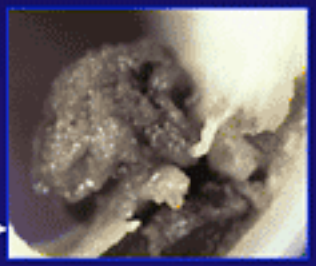

Libby, P. Circ. 2001:103:1718-1720.

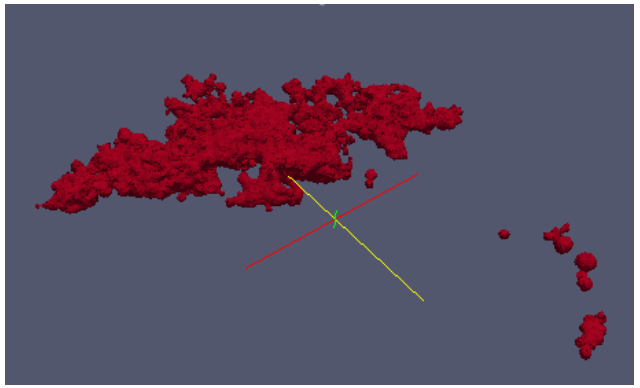

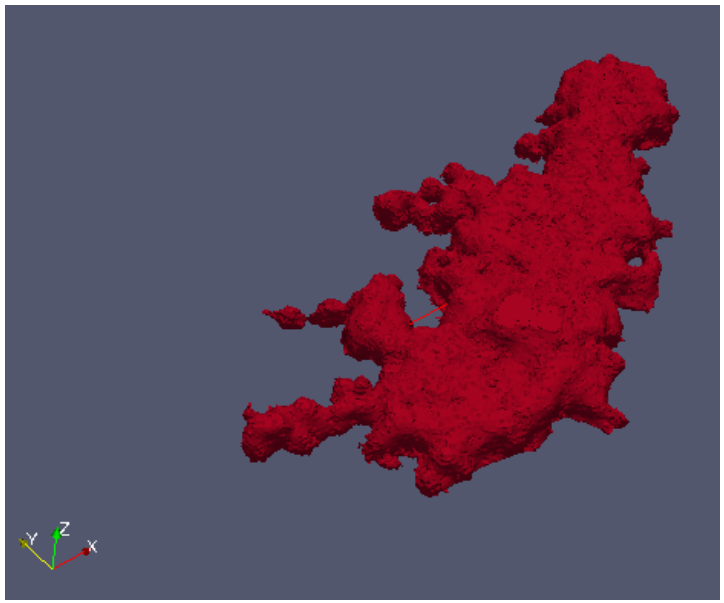

Effect of haemodynamic forces on thrombi geometry

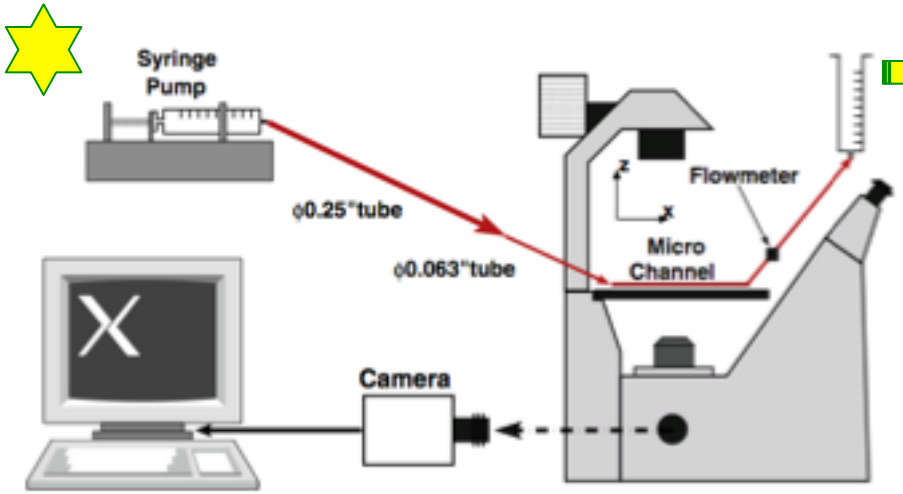

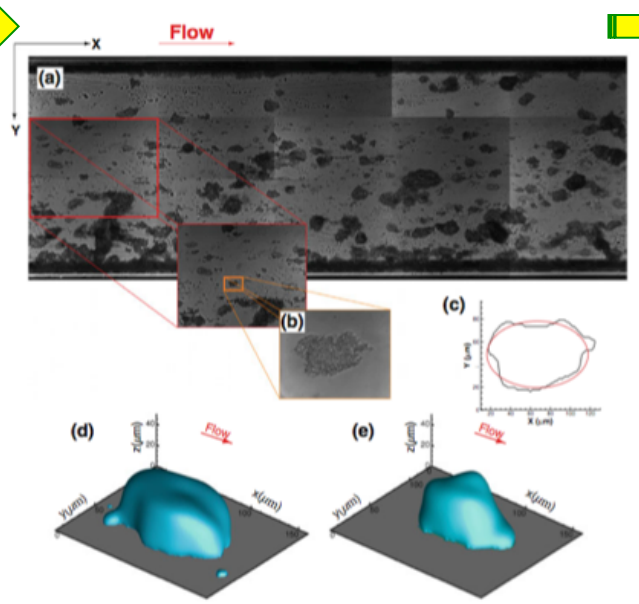

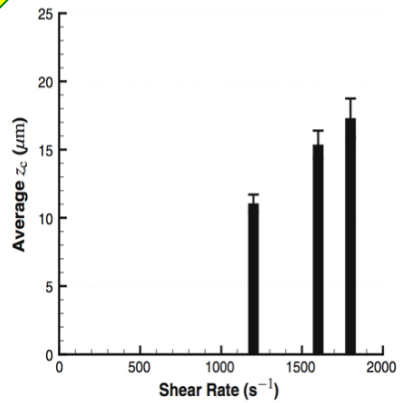

Average centroid height (z_c) of mature platelet aggregations increases with shear rate

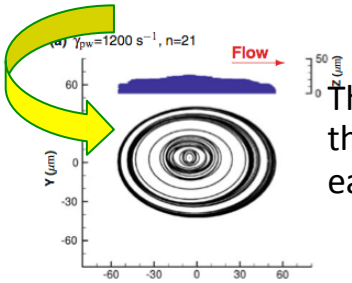

The three-dimensional profiles for the average platelet aggregations at each shear rate

Measurement of platelet aggregation geometries using bright field scanning microscopy and image reconstruction

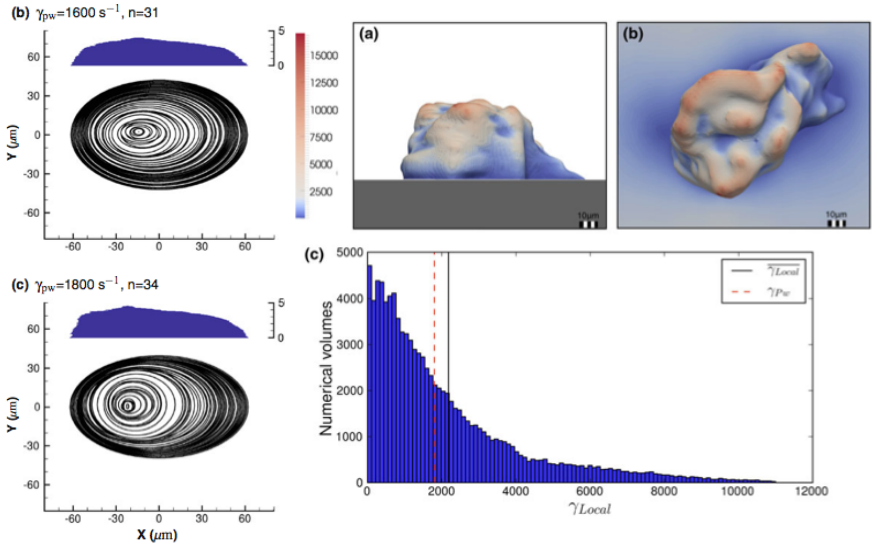

Local shear rate distribution around a representative mature platelet aggregation

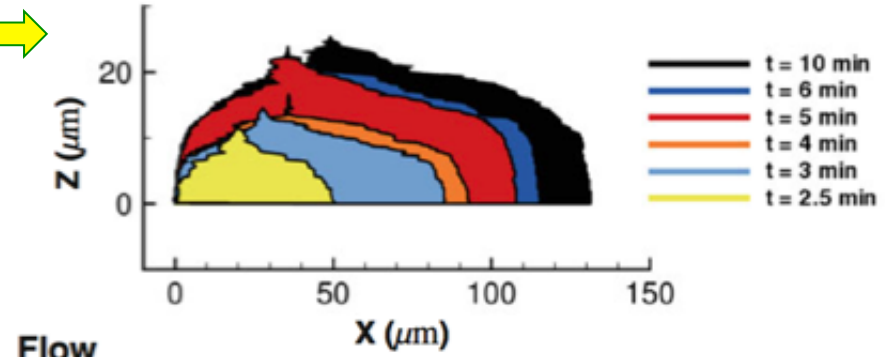

Variation of average cross-sectional area with exposure time

Tolouei, E., Butler, C.J., Fouras, A., Ryan, K., Sheard, G.J. & Carberry, J. (2011) *Effect of hemodynamic forces on thrombi geometry*. Annals of Biomedical Engineering. 39 (5), 1403-1413.

Extending to 3-Dimensional analysis of *in vivo* flows

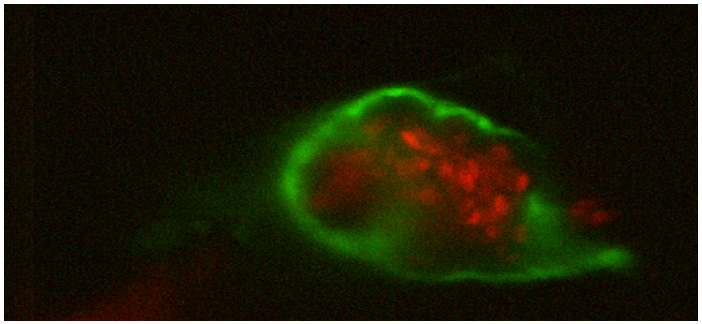

Zebra fish heart: tissue, blood

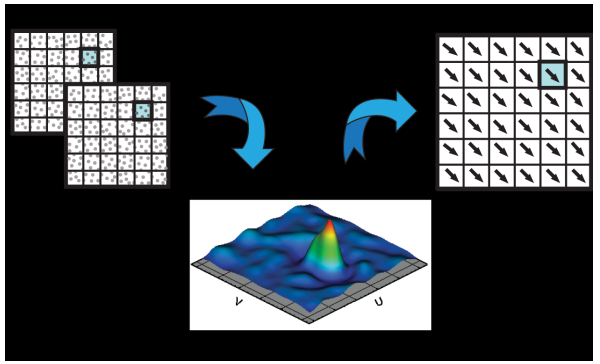

Particle Image Velocimetry

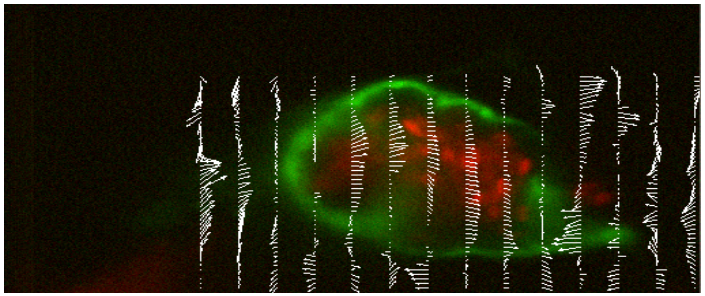

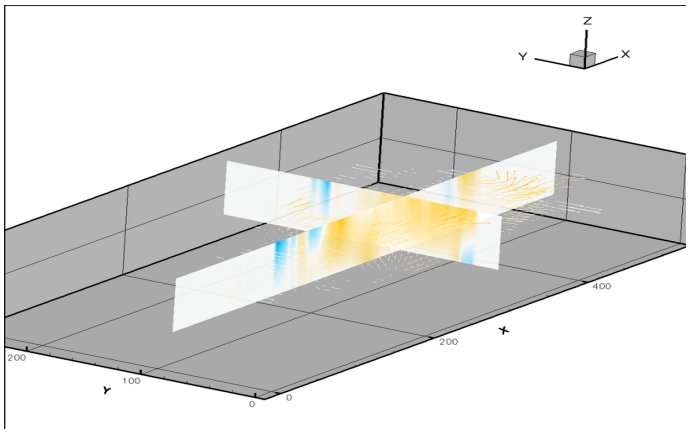

2d -> 3d velocity fields

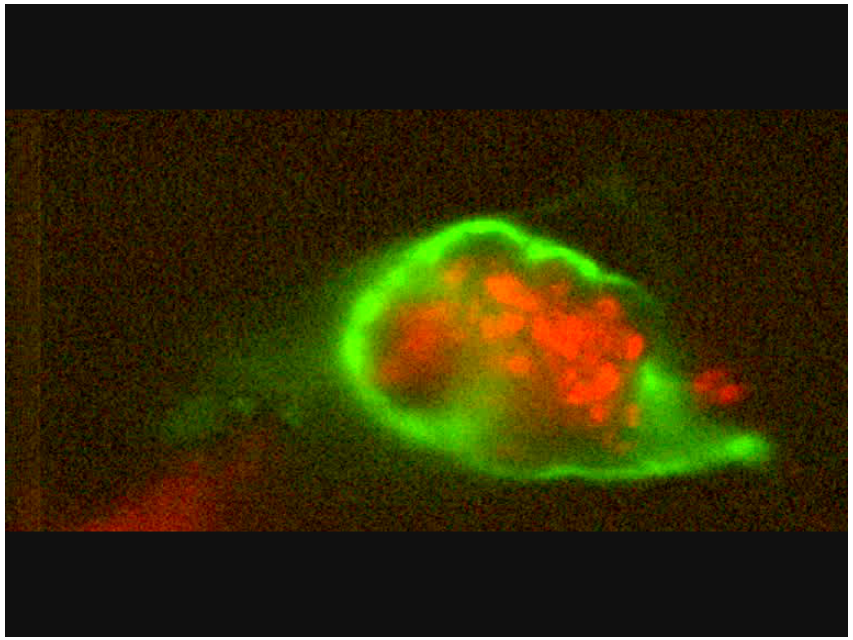

Small, beating, compliant, non-Newtonian blood

Outline of the Presentation

- Context of current research
- Atherosclerosis overview
- Computed Tomographic X-ray Velocimetry
  - Synthetic: Stenosis
  - In vitro: Thrombi
  - In vivo: Heart
- CFD
  - Idealised stenoses
  - Mouse aorta
- Conclusions

CFD in idealised stenosed vessels – see Poster by Griffith et al.

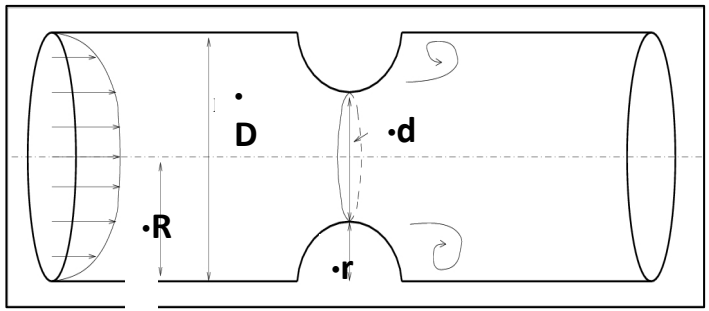

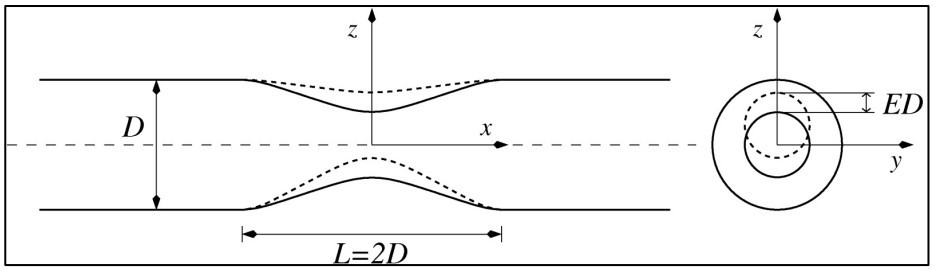

Steady inflow

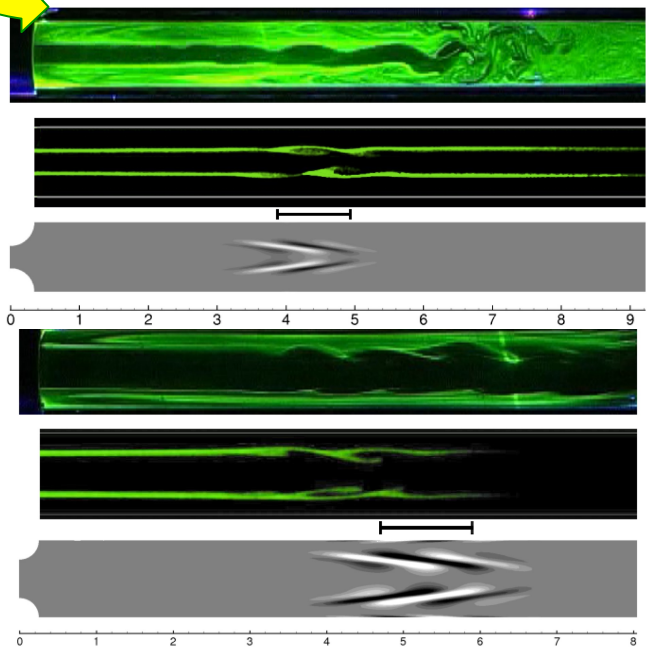

Pulsed inflow

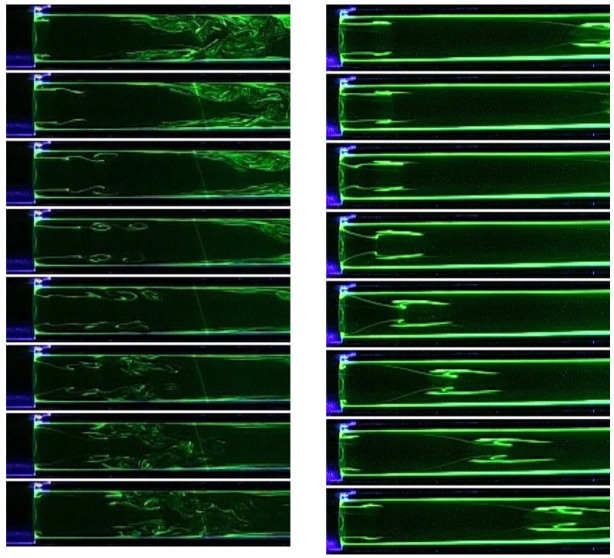

Eccentric stenosis

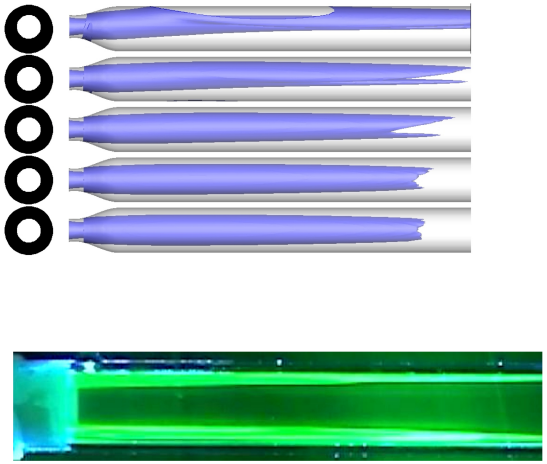

Griffith, M.D., Leweke, T., Thompson, M.C. & Hourigan, K. 2008 Steady inlet flow in stenotic geometries: convective and absolute instabilities. *Journal of Fluid Mechanics* **616**, 111-133.

Griffith, M.D., Leweke, T., Thompson, M.C. & Hourigan, K. 2009 Pulsatile flow in stenotic geometries: flow behaviour and stability. *Journal of Fluid Mechanics* **622**, 291-320.

Griffith, M.D., Thompson, M.C., Leweke, T. & Hourigan, K. 2010 Convective instability in steady stenotic flow: optimal transient growth and experimental observation. *Journal of Fluid Mechanics* **655**, 504-514.

Outline of the Presentation

- Context of current research
- Atherosclerosis overview
- Computed Tomographic X-ray Velocimetry
    - Synthetic: Stenosis
    - In vitro: Thrombi
    - In vivo: Heart
- CFD
    - Idealised stenoses
    - ⇨ Mouse aorta
- Conclusions

CFD in the model from a mouse

Mouse aorta geometry

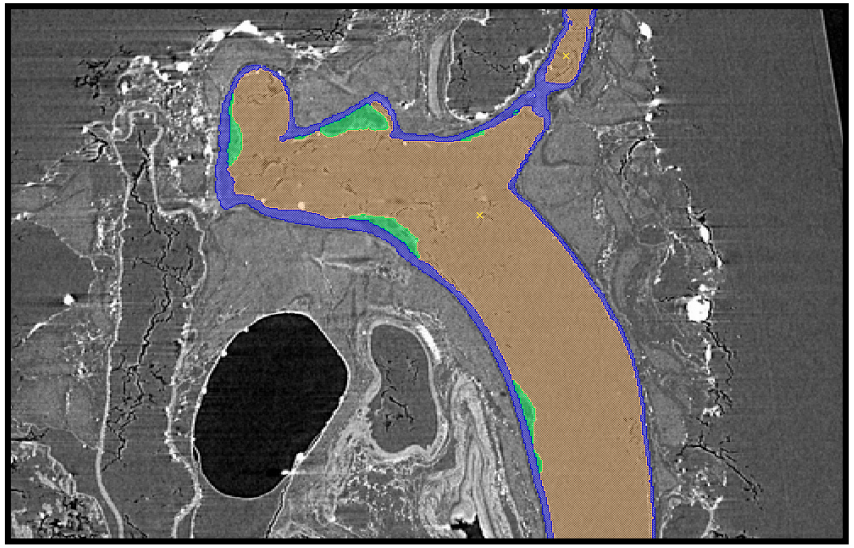

Two-dimensional slice in Avizo showing a section of the aortic arch of an Apo E-deficient mouse. The image has been segmented, vessel (blue), plaque (green) and lumen (brown).

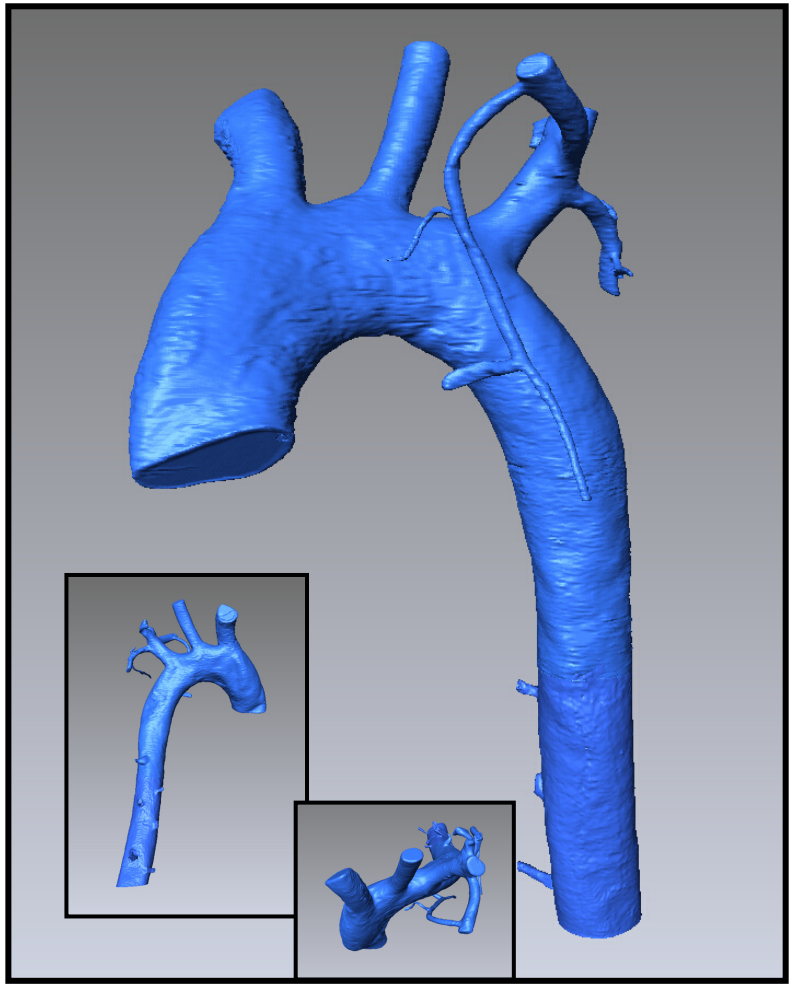

Mouse aorta geometry.

Vessel geometry: CAD

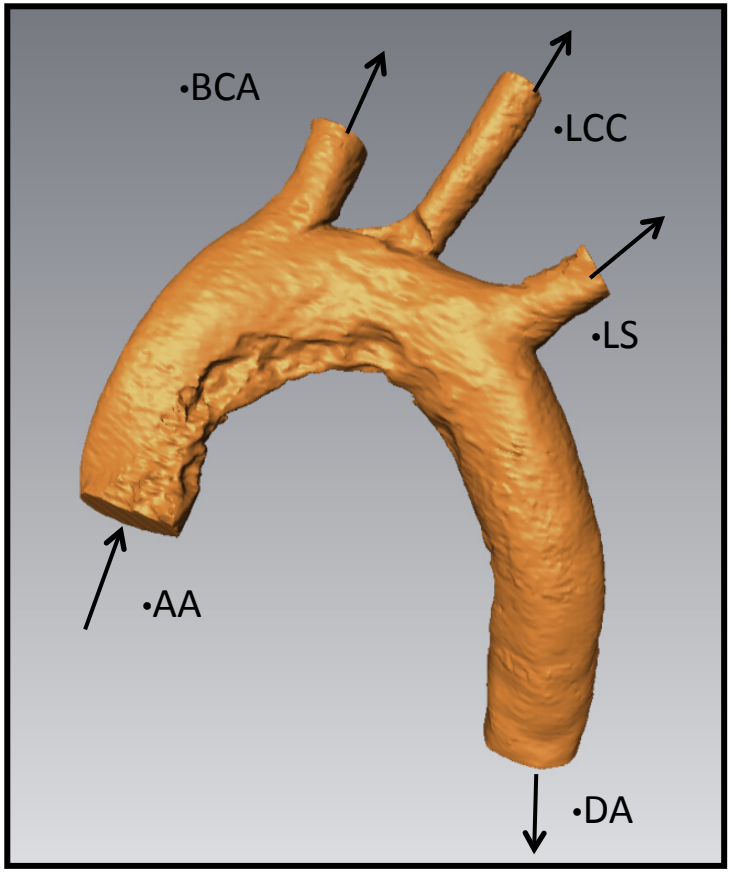

The lumen of the vessel which has been segmented and cropped, ready for meshing in ICEM CFD.

	Ascending Aorta (AA)	Brachiocephalic Artery (BCA)	Left Common Carotid Artery (LCC)	Left Subclavian Artery (LS)	Descending Aorta (DA)
Diameter, D (mm)	0.83	0.56	0.33	0.38	0.82
Flow Rate, Q (mL/min) [7]	12.02	1.87	1.35	1.06	7.74
Reynolds Number, Re	95	22	27	18	62

Dimensions of the aorta and its main branches measured from the reconstructed three-dimensional geometry. The flow rates used as boundary conditions were obtained from Huo et al. (2008).

Plaque locations

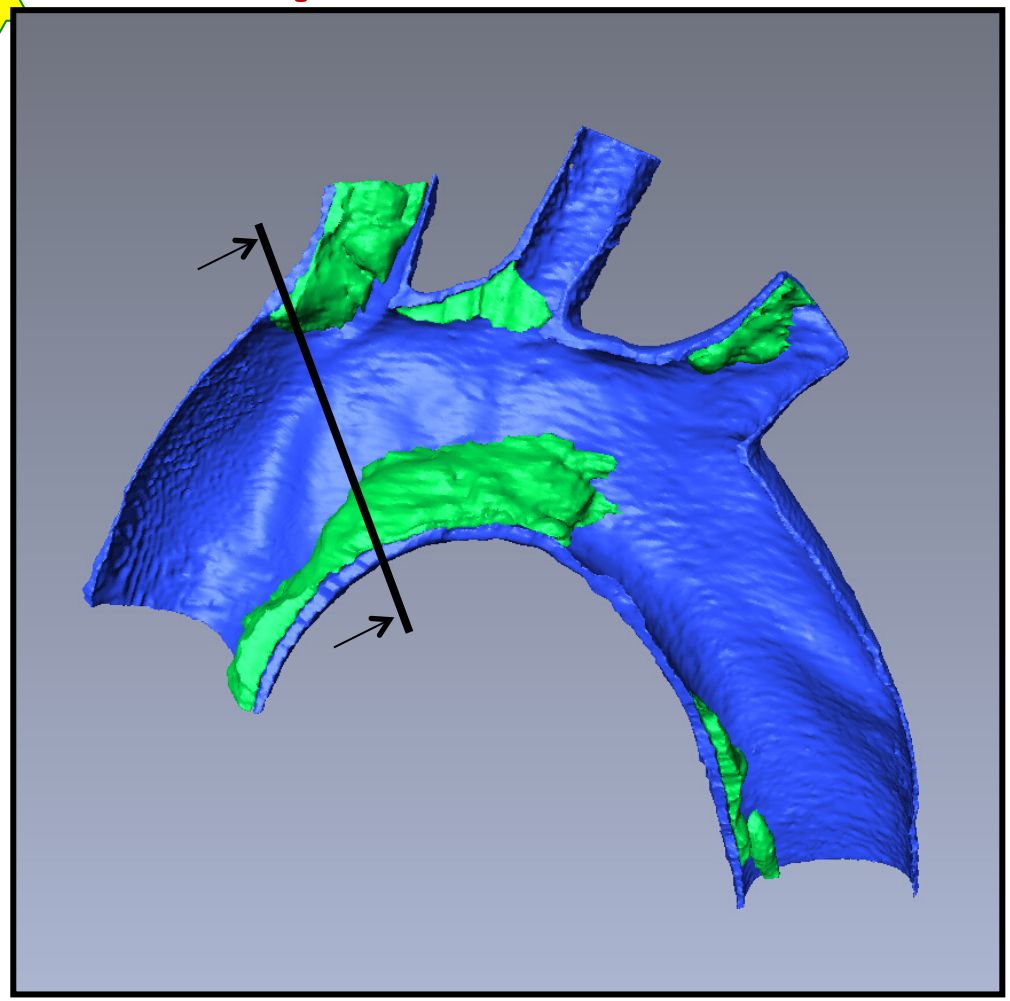

Section of the ApoE-deficient mouse aorta demonstrating the location of the plaques (green) on the inner curvature of the aorta and on the upstream side of the three main branch points.

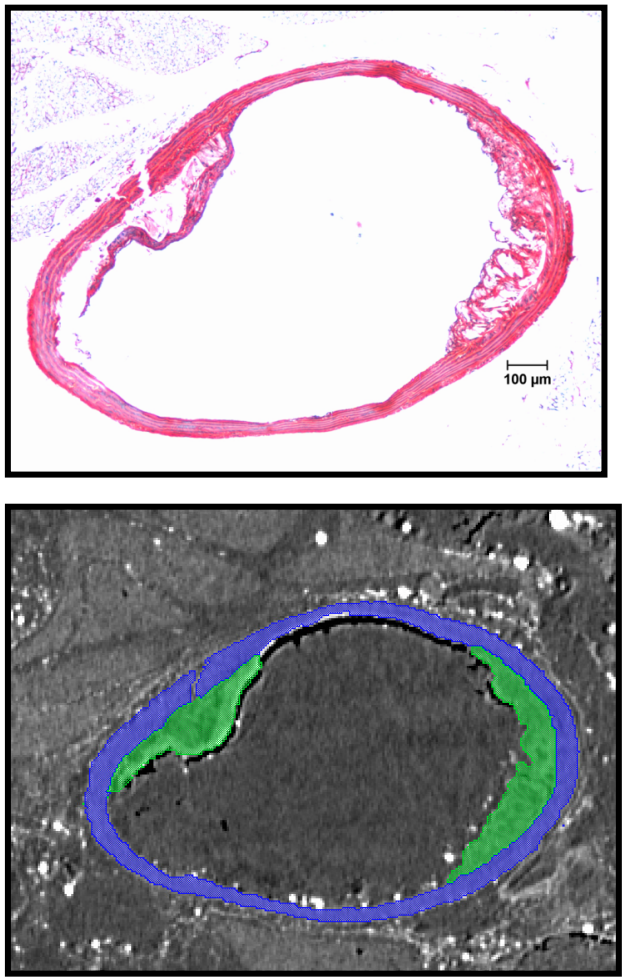

a) Histology of a cross-section of the AA and BCATwo plaques are visible, one with a well defined fibrous cap (provided by J. Armitage).
b) Related two-dimensional slice in Avizo with the wall and plaque segmented.

Surface pressure

Plaque present

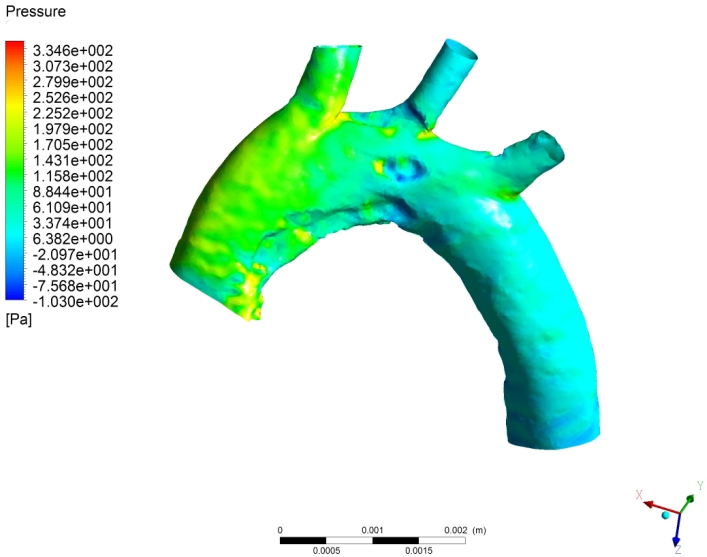

Plaque “removed”

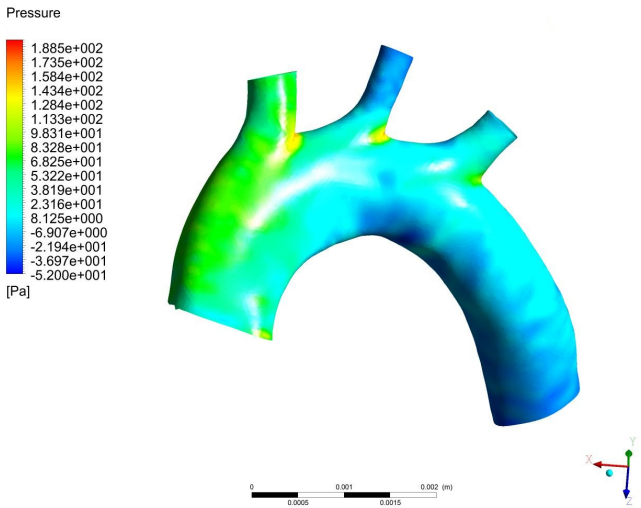

Wall shear stress

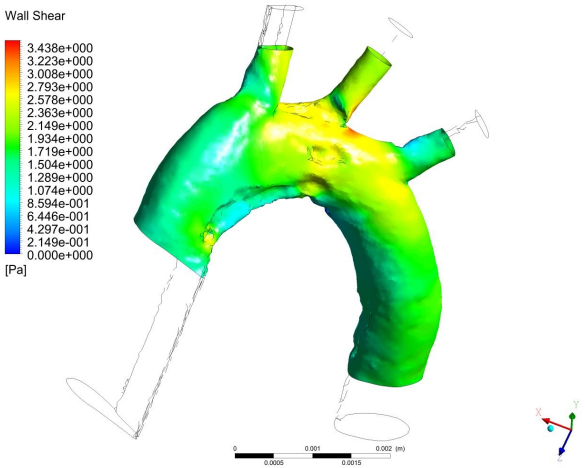

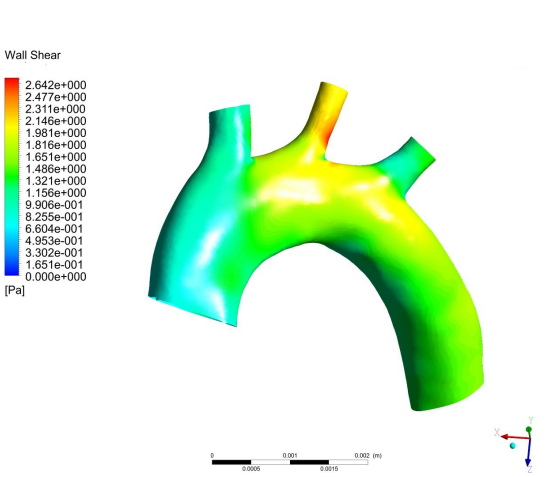

Wall shear stress (exaggerated contours)

Plaque present

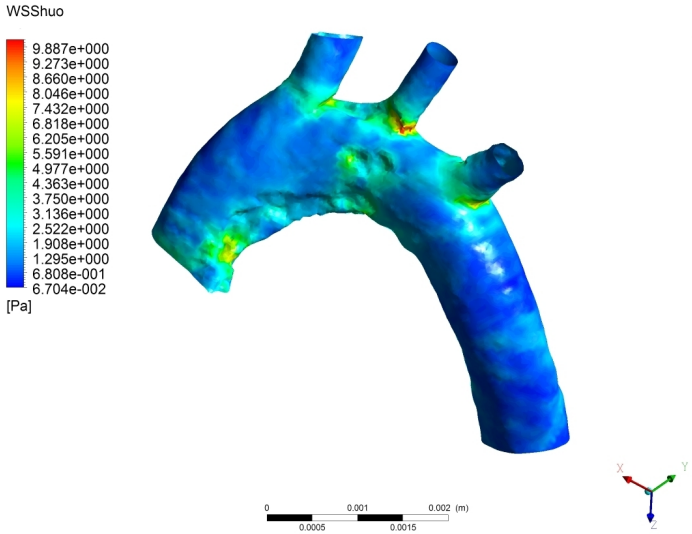

Plaque “removed”

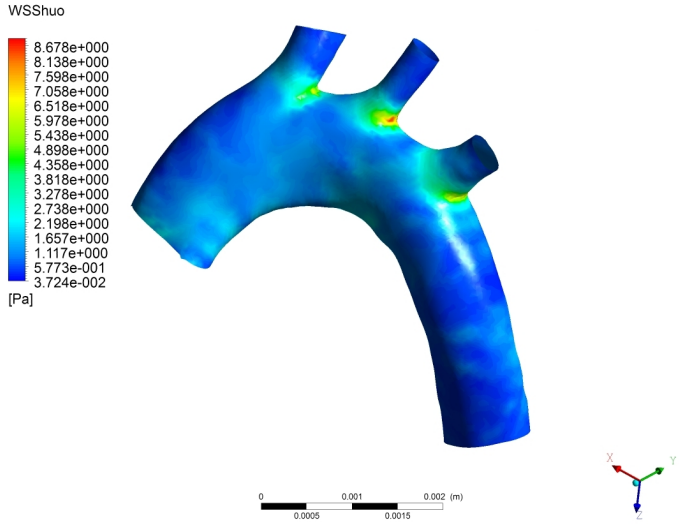

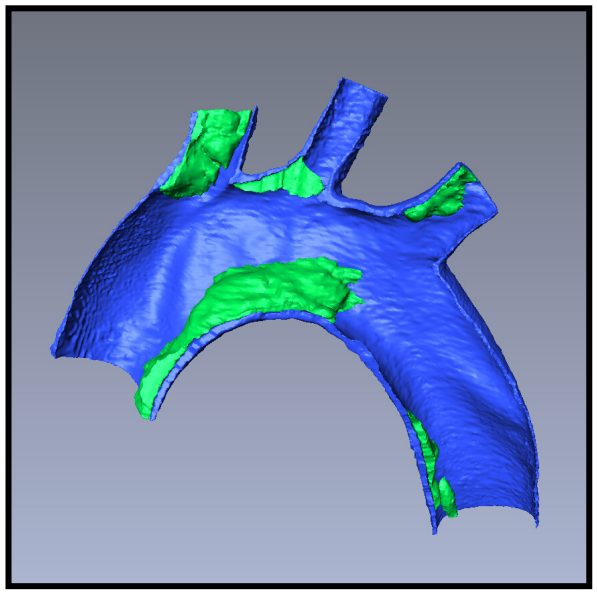

c.f. plaque locations

Outline of the Presentation

- Context of current research
- Atherosclerosis overview
- Computed Tomographic X-ray Velocimetry
    - Synthetic: Stenosis
    - In vitro: Thrombi
    - In vivo: Heart
- CFD
    - Idealised stenoses
    - Mouse aorta
- Conclusions

Conclusions

- X-ray CT Velocimetry + CFD can be used to determine tissue geometries, blood flow velocity fields, WSS, etc
- In accordance with the literature, plaques were found to develop on the inner curvature of the aortic arch and the upstream side of the main branches in Apo E-deficient mice
- The WSS results are consistent with those found by others in arteries without plaque
- As an extension to previous work, the flow around plaque has been investigated, with altered WSS distributions observed
- Work is in progress looking at the deformation of the arterial wall and plaque by incorporating the elastic properties of the materials (coupled solver, AFM, Biodynamic tester)
- X-ray CT+Velocimetry + *in vivo*, functional nanoparticles will also be investigated
- Part of a broader program in lung/brain/cardiovascular, imaging, cfd, nanotechology, drug delivery, devices, ….

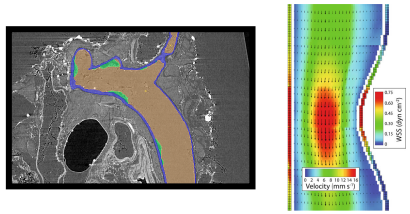

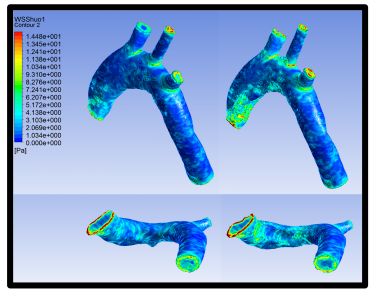

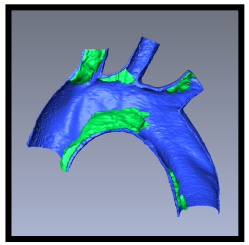

Acknowledgements

MONASH University

Baker IDI
HEART & DIABETES INSTITUTE

Australian Synchrotron

Australian Government
Australian Research Council

Swiss Light Source

Multidisciplinary research – one needs to wear many hats

Myocardial Infarction

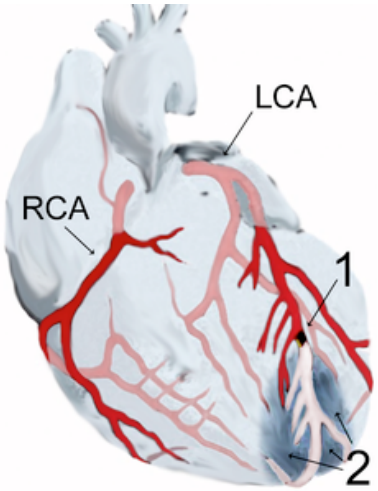

Wikipedia

- Results from the interruption of blood supply to a part of the heart, causing heart cells to die
- Most commonly due to occlusion (blockage) of a coronary artery following the rupture of a vulnerable atherosclerotic plaque
- vulnerable plaque rupture causes as many as 85% of all heart attacks.

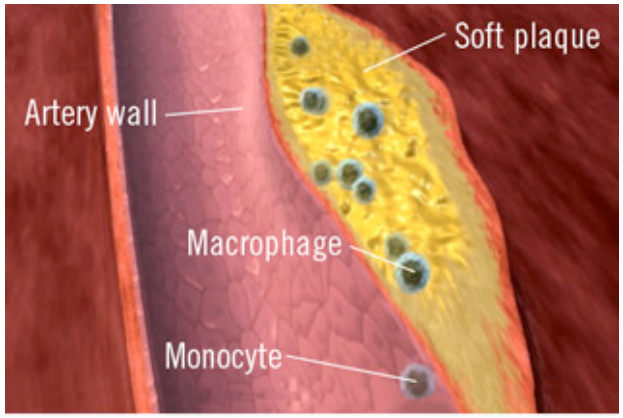

- As cholesterols are absorbed by the artery, proteins called "cytokines" are released. The cytokines cause inflammation and make the arterial wall sticky, resulting in the attraction of immune-system cells to the area. The immune-system cells are called "monocytes."
- When the monocytes enter the arterial wall, they differentiate into "macrophage" cells and begin to absorb fat droplets. Over time, these fat-filled cells form a plaque – what researchers now call "vulnerable plaque.

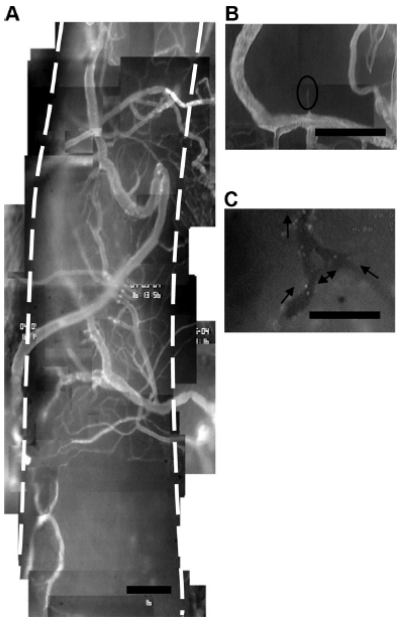

Microvessels in atherosclerosis as important entry pathways for leukocytes to lesions.

Eriksson, Circulation 2011, 124:2129-2138

Computed Tomographic X-ray Velocimetry of Biofluid Flows

2D

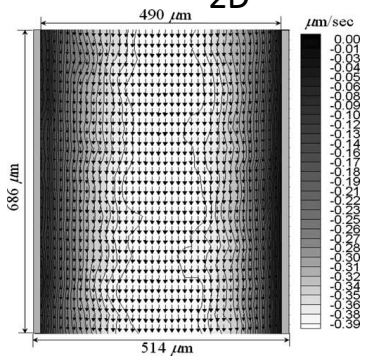

Kim GB, Lee SJ (2006) *X-ray PIV measurements of blood flows without tracer particles*. Exp Fluids 41:195-2006

Axisymmetric

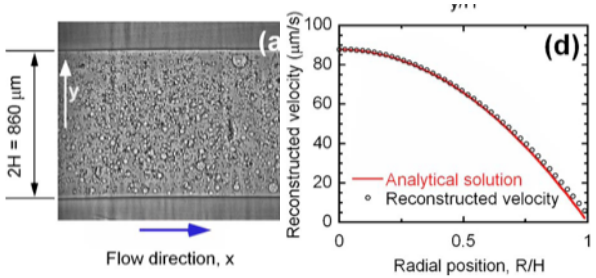

Im KS, Fezzaa K, Wang YJ, Liu X, Wang J, Lai MC (2007) *Particle tracking velocimetry using fast X-ray phase-contrast imaging*. Appl Phys Lett 90: Artn 091919

3D, planar symmetry assumed

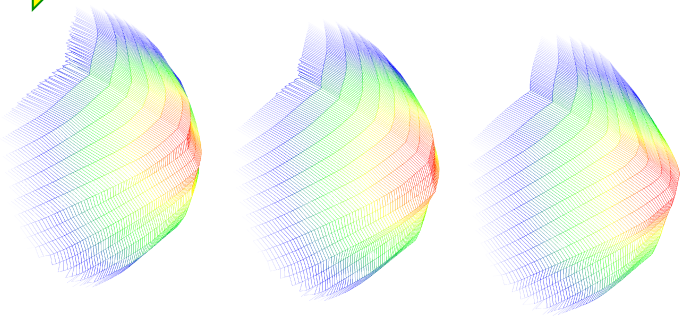

Fouras A, Dusting J, Lewis R, Hourigan K (2007) *Three-dimensional synchrotron X-ray particle image velocimetry*. J Appl Phys 102: Artn 064916

Axisymmetric

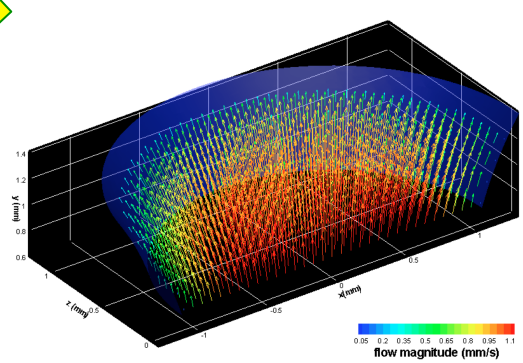

Irvine SC, Paganin DM, Jamison A, Dubsky S, Fouras A (2010*) Vector tomographic X-ray phase contrast velocimetry utilizing dynamic blood speckle*. Opt Express 18:2368-2379

3D, Axisymmetric

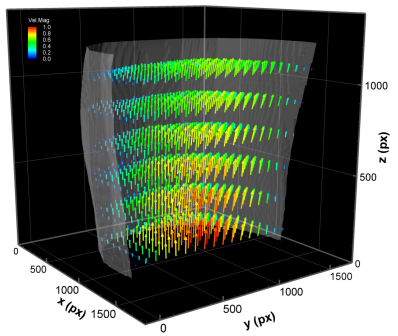

Dubsky, S., R.A. Jamison, S.C. Irvine, K.K.W. Siu, K. Hourigan, and A. Fouras, *Computed tomographic X-ray velocimetry.* Applied Physics Letters, 2010. **96**(2)

	Ascending Aorta (AA)	Brachiocephalic Artery (BCA)	Left Common Carotid Artery (LCC)	Left Subclavian Artery (LS)	Descending Aorta (DA)
Flow Rate, Q (mL/min) [7]	12.02	1.87	1.35	1.06	7.74
Diameter, D (mm) [7]	1.3	0.85	0.64	0.64	-
Reynolds Number [7]	61	14	14	11	-
Experimental Diameter, D (mm)	0.83	0.56	0.33	0.38	0.82
Experimental Reynolds Number, Re	95	22	27	18	62

Table 1: Comparison of diameter and Reynold's number from experimental findings and the values stated in Huo et al (2008). The experimental dimensions of the aorta and its main branches were measured from the reconstructed three-dimensional geometry. The flow rates used as boundary conditions were obtained from Huo et al (2008). In the Reynolds number calculations ($Re=\rho QD/(6x10^6 A\mu)$), Q is the flow rate, A is the surface area and D is the equivalent diameter of the artery. The density (ρ) is 1235kg/m^3 and the dynamic viscosity (μ) is 0.004Pa.s.

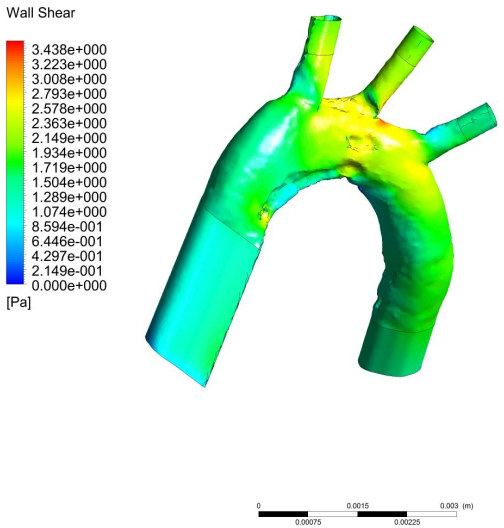
Wall Shear
3.438e+000
3.223e+000
3.008e+000
2.793e+000
2.578e+000
2.363e+000
2.149e+000
1.934e+000
1.719e+000
1.504e+000
1.289e+000
1.074e+000
8.594e-001
6.446e-001
4.297e-001
2.149e-001
0.000e+000
[Pa]
0
0.0015
0.003 (m)
0.00075
0.00225
X
Y
Z

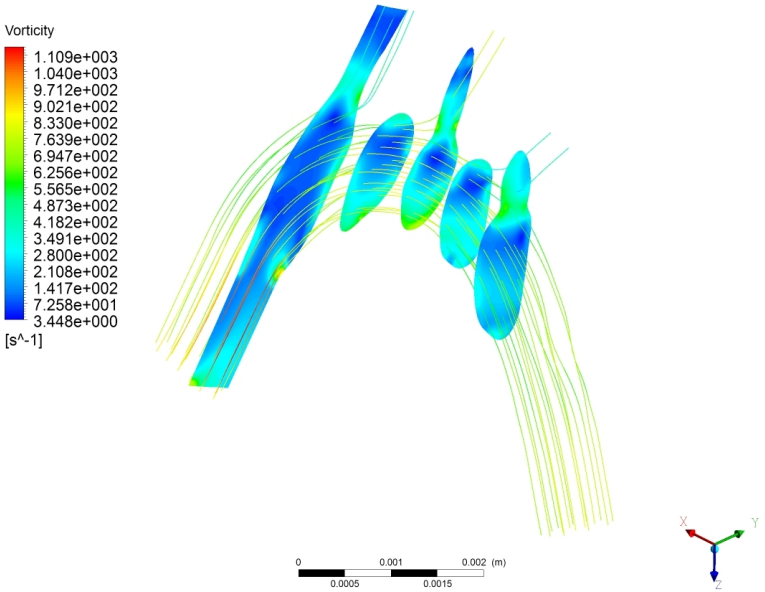
Vorticity
1.109e+003
1.040e+003
9.712e+002
9.021e+002
8.330e+002
7.639e+002
6.947e+002
6.256e+002
5.565e+002
4.873e+002
4.182e+002
3.491e+002
2.800e+002
2.108e+002
1.417e+002
7.258e+001
3.448e+000
[s^-1]
0
0.001
0.002 (m)
0.0005
0.0015
X
Y
Z

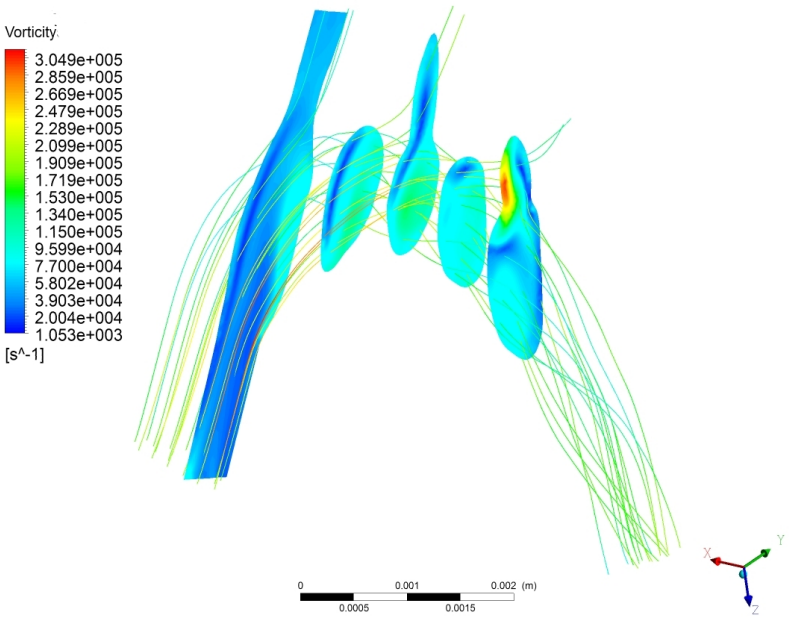
Vorticity
3.049e+005
2.859e+005
2.669e+005
2.479e+005
2.289e+005
2.099e+005
1.909e+005
1.719e+005
1.530e+005
1.340e+005
1.150e+005
9.599e+004
7.700e+004
5.802e+004
3.903e+004
2.004e+004
1.053e+003
[s^-1]
0
0.001
0.002 (m)
0.0005
0.0015
X
Y
Z

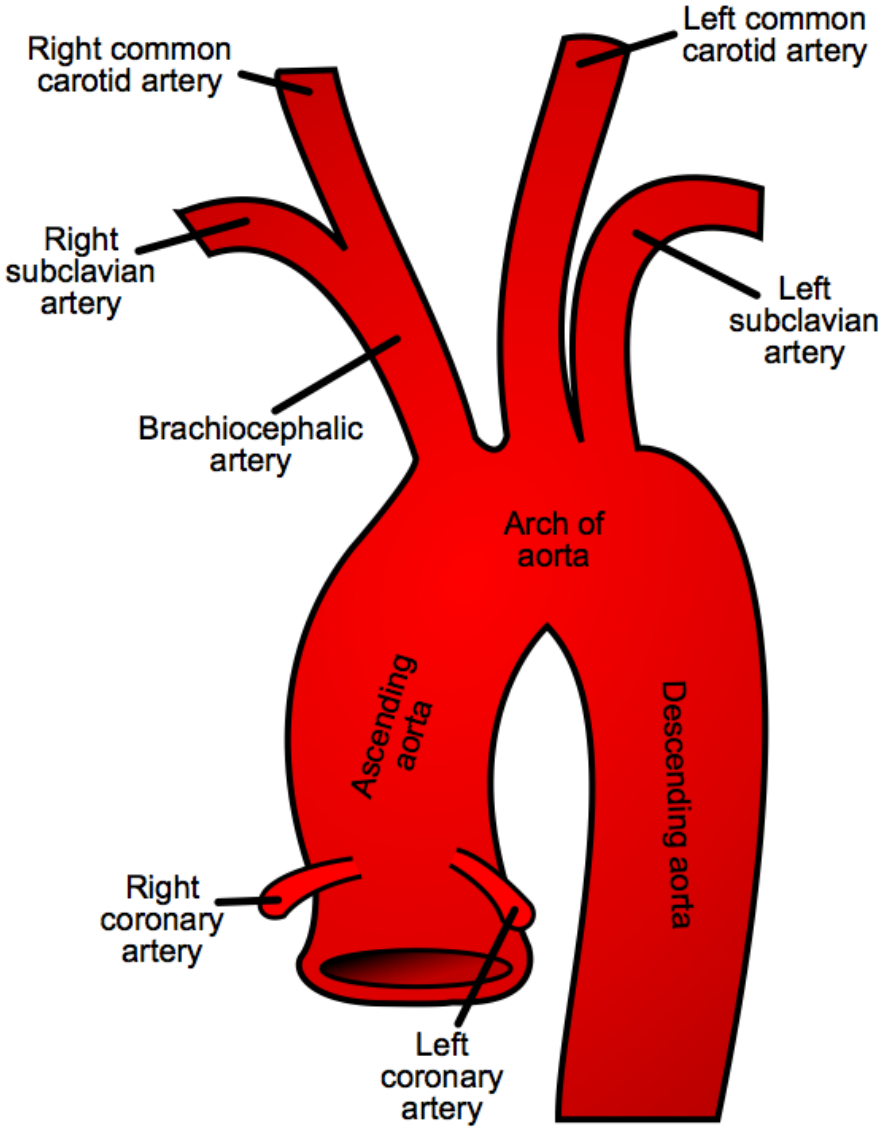

- http://upload.wikimedia.org/wikipedia/commons/thumb/e/e6/Gray506.svg/250px-Gray506.svg.png